

## Further Study of the Linear Trinickel(II) Complex of Dipyriddyamide

Rodolphe Clérac,<sup>†</sup> F. Albert Cotton,<sup>\*,‡</sup> Kim R. Dunbar,<sup>†</sup> Carlos A. Murillo,<sup>\*,‡,§</sup> Isabel Pascual,<sup>‡</sup> and Xiaoping Wang<sup>‡</sup>

Department of Chemistry and The Center for Fundamental Material Research, Michigan State University, East Lansing, Michigan 48824, Laboratory for Molecular Structure and Bonding, Department of Chemistry, Texas A&M University, P.O. Box 30012, College Station, Texas 77842-3012, and Department of Chemistry, University of Costa Rica, Ciudad Universitaria, Costa Rica

Received January 6, 1999

The title compound,  $\text{Ni}_3(\text{dpa})_4\text{Cl}_2$  (dpa = di(2-pyridyl)amido anion), first reported 30 years ago, structurally characterized in 1991, has been obtained in two new crystal forms,  $\text{Ni}_3(\text{dpa})_4\text{Cl}_2 \cdot 2\text{CH}_2\text{Cl}_2$  (tetragonal, space group  $I4$ , with  $a = 27.3046(7)$  Å,  $c = 12.2452(2)$  Å,  $Z = 8$ ) and  $\text{Ni}_3(\text{dpa})_4\text{Cl}_2 \cdot \text{THF}$  (orthorhombic, space group  $Pccn$ , with  $a = 12.673(1)$  Å,  $b = 14.138(3)$  Å,  $c = 23.890(2)$  Å,  $Z = 4$ ). They have been examined structurally, and the magnetic properties of one of them determined from 2 to 300 K. Also the proton NMR spectrum has been recorded. These data allow the following conclusions to be drawn: (1) the molecular structure is invariant in the three crystalline forms and has a symmetrical chain of nickel atoms, (2) the terminal metal atoms each have two unpaired electrons, while the central one is typical of diamagnetic square-planar  $\text{Ni}^{\text{II}}$  complexes, (3) the magnetic moments of the two terminal nickel(II) ions display antiferromagnetic coupling, with  $2J = -108 \text{ cm}^{-1}$ , and (4) the  $\text{Ni}_3$  chain remains symmetrical in solution.

## Introduction

The purple compound  $\text{Ni}_3(\text{dpa})_4\text{Cl}_2$  (dpa = di(2-pyridyl)-amido anion) was first reported in 1968.<sup>1</sup> It was shown to be paramagnetic and trinuclear, but the structure was not determined. A structure was proposed, but in 1991 this proposal was shown to be incorrect, and the correct structure, in which there is a linear chain,  $\text{Cl}-\text{Ni}-\text{Ni}-\text{Ni}-\text{Cl}$ , surrounded by a spiral set of four dpa ligands, was described.<sup>2</sup> Subsequently, similar compounds containing Cu, Co, Cr, Ru, and Rh atoms have also been reported.<sup>3</sup>

Because of our interest in the chemistry of and bonding in  $\text{M}_3(\text{dpa})_4\text{X}_2$  compounds generally, it was desirable to characterize  $\text{Ni}_3(\text{dpa})_4\text{Cl}_2$  further. We began with a more straight-forward method of preparation than that previously used,<sup>1,2</sup> which led to two different crystal forms from the one previously studied crystallographically.<sup>2</sup> The magnetic properties were studied from 2 to 300 K, and the  $^1\text{H}$  NMR spectrum, which shows large downfield contact shifts, was measured in dichloromethane solution.

## Experimental Section

**Materials.** All manipulations were performed under an atmosphere of nitrogen using standard Schlenk techniques. Solvents were purified by conventional methods and were freshly distilled under nitrogen prior to use. Anhydrous nickel chloride, di(2-pyridyl)amine (Hdpa), and methylolithium (1.0 M in THF) were purchased from Aldrich Chemical Co.; Hdpa was resublimed and  $\text{NiCl}_2$  was refluxed with  $\text{SOCl}_2$  before use, but other chemicals were used as received.

**Physical Measurements.** The IR spectrum was recorded on a Perkin-Elmer 16PC FT-IR spectrophotometer as KBr pellet. The proton NMR spectrum was recorded on a Varian Unity 300 spectrometer at 299.96 MHz; chemical shifts are referenced to TMS (0.00 ppm). The magnetic susceptibility data were collected on a Quantum Design, model MPMS, SQUID (superconducting quantum interference device) housed in the Department of Physics and Astronomy at Michigan State University. Data were collected from 2 to 300 K at a field of 2000 G.

**Preparation of  $\text{Ni}_3(\text{dpa})_4\text{Cl}_2 \cdot 2\text{CH}_2\text{Cl}_2$ .** A solution of Lidpa was prepared by adding 4.0 mL of 1.0 M methylolithium to a solution of Hdpa (0.685 g, 4.0 mmol) in THF at  $-78^\circ\text{C}$ . The Lidpa suspension was allowed to return to ambient temperature. It was then transferred to a round-bottomed flask containing  $\text{NiCl}_2$  (0.415 g, 3.2 mmol). The resulting brown mixture was refluxed for 6 h to give a purple suspension, which was cooled to room temperature and filtered. The remaining dark-purple solid was extracted with  $\text{CH}_2\text{Cl}_2$  (30 mL). Slow diffusion of hexanes (30 mL) into the  $\text{CH}_2\text{Cl}_2$  solution gave prism-shaped purple crystals. Additional product was obtained from workup of the filtrate. The solvent in the filtrate was removed under reduced pressure, and the remaining solid was partially dissolved in  $\text{CH}_2\text{Cl}_2$ . This solution was filtered, and the filtrate was layered with hexanes. Purple crystals from both solutions were collected and washed with hexanes. Yield: 0.66 g, 60.2%. Anal. Calcd for  $\text{C}_{42}\text{H}_{36}\text{N}_{12}\text{Cl}_6\text{Ni}_3$ : C, 45.96; H, 3.31; N, 15.31. Found: C, 45.58; H, 3.21; N, 14.74.  $^1\text{H}$  NMR ( $\text{CD}_2\text{Cl}_2$ ):  $\delta$  9.08, 15.69, 32.32, 48.79. IR (KBr pellet,  $\text{cm}^{-1}$ ): 1603 (s), 1592 (s), 1550 (m), 1466 (s), 1458 (sh, s), 1421 (s), 1364 (s), 1353 (s), 1311 (m), 1281 (w), 1242 (w), 1152 (m), 1052 (w), 1014 (m), 926 (w), 893 (w), 764 (m), 740 (m), 730 (m), 639(w), 518(w), 428 (w).

**Preparation of  $\text{Ni}_3(\text{dpa})_4\text{Cl}_2 \cdot \text{THF}$ .** The procedure was essentially the same as that just described. The THF-containing crystals were grown from the filtrate obtained after separation of the dark-purple solid which had been layered with hexanes. After 24 h, well-formed, red-black crystals appeared.

**X-ray Structure Determinations.** Geometric and intensity data for  $\text{Ni}_3(\text{dpa})_4\text{Cl}_2 \cdot 2\text{CH}_2\text{Cl}_2$  were gathered at  $-60^\circ\text{C}$  on a Nonius FAST area detector system, utilizing the software program MADNES.<sup>4</sup> Unit cell refinement utilized 250 strong reflections in the  $2\theta$  range of  $18.1-41.8^\circ$ . The cell dimensions and Laue group were confirmed by axial images. All data were corrected for Lorentz and polarization effects.

\* To whom correspondence should be addressed.

<sup>†</sup> Michigan State University.

<sup>‡</sup> Texas A&M University.

<sup>§</sup> University of Costa Rica.

(1) Hurley, T. J.; Robinson, M. A. *Inorg. Chem.* **1968**, 7, 33.

(2) Aduldech, S.; Hathaway, B. J. *Chem. Soc., Dalton Trans.* **1991**, 993.

(3) For references to all of these compounds, see: Clérac, R.; Cotton, F. A.; Daniels, L. M.; Dunbar, K. R.; Murillo, C. A.; Pascual, I. *Inorg. Chem.*, submitted.

**Table 1.** Crystal and Structure Refinement Data for  $\text{Ni}_3(\text{dpa})_4\text{Cl}_2 \cdot 2\text{CH}_2\text{Cl}_2$  (**2**) and  $\text{Ni}_3(\text{dpa})_4\text{Cl}_2 \cdot \text{THF}$  (**3**)

	<b>2</b>	<b>3</b>
formula	$\text{C}_{42}\text{H}_{36}\text{Cl}_6\text{N}_{12}\text{Ni}_3$	$\text{C}_{44}\text{H}_{40}\text{Cl}_2\text{N}_{12}\text{Ni}_3\text{O}$
fw	1097.66	999.91
space group	<i>I</i> 4	<i>Pccn</i>
<i>a</i> , Å	27.3046(7)	12.673(1)
<i>b</i> , Å	27.3046(7)	14.138(3)
<i>c</i> , Å	12.2452(2)	23.890(2)
<i>V</i> , Å <sup>3</sup>	9129.3(4)	4280.4(9)
<i>Z</i>	8	4
$\rho_{\text{calc}}$ , g cm <sup>-3</sup>	1.597	1.552
$\mu$ , mm <sup>-1</sup>	1.623	1.483
radiation (Mo K $\alpha$ ), Å	0.71073	0.71073
temperature, K	213(2)	173(2)
$R1^a$ $wR2^b$ [ $I > 2\sigma(I)$ ]	0.039, 0.098	0.046, 0.110
$R1^a$ $wR2^b$ (all data)	0.041, 0.100	0.107, 0.131

<sup>a</sup>  $R1 = \sum ||F_o| - |F_c|| / \sum |F_o|$ . <sup>b</sup>  $wR2 = [\sum w(F_o^2 - F_c^2)^2 / \sum w(F_o^2)^2]^{1/2}$ .

**Table 2.** Selected Interatomic Distances (Å) for  $\text{Ni}_3(\text{dpa})_4\text{Cl}_2 \cdot 2\text{CH}_2\text{Cl}_2$  (**2**)

Ni(1)···Ni(2)	2.4386(9)	Ni(2)···Ni(3)	2.422(1)
Ni(1)–Cl(1)	2.348(2)	Ni(3)–Cl(2)	2.336(2)
Ni(1)–N(1)	2.086(4)	Ni(2)–N(2)	1.894(4)
Ni(3)–N(3)	2.084(5)	Ni(1)–N(4)	2.101(5)
Ni(2)–N(5)	1.890(4)	Ni(3)–N(6)	2.095(5)
Ni(3)–N(7)	2.094(5)	Ni(2)–N(8)	1.883(5)
Ni(1)–N(9)	2.104(5)	Ni(3)–N(10)	2.079(5)
Ni(2)–N(11)	1.898(4)	Ni(1)–N(12)	2.099(5)

**Table 3.** Selected Interatomic Distances (Å) for  $\text{Ni}_3(\text{dpa})_4\text{Cl}_2 \cdot \text{THF}$  (**3**)

Ni(1)···Ni(2)	2.4172(8)	Ni(1)–Cl(1)	2.334(2)
Ni(1)–N(1)	2.099(5)	Ni(1)–N(4)	2.086(5)
Ni(2)–N(2)	1.889(5)	Ni(2)–N(5)	1.897(5)
Ni(1)–N(3)	2.080(5)	Ni(1)–N(6)	2.063(5)

Data were processed into SHELX format using the program PROCOR.<sup>5</sup> The positions of the heavy atoms were located in direct methods E-maps using the software solution program in SHELXTL.<sup>6</sup> Subsequent cycles of least-squares refinement followed by difference Fourier synthesis revealed the positions of the remaining non-hydrogen atoms. Hydrogen atoms were placed in idealized calculated positions. Details of data collection and refinement are given in Table 1. Selected atomic distances are provided in Table 2.

Geometric and intensity data for  $\text{Ni}_3(\text{dpa})_4\text{Cl}_2 \cdot \text{THF}$  were collected on a Nonius CAD4 4-circle diffractometer. Preliminary examination revealed a primitive orthorhombic cell, and systematic absences corresponded to space group *Pccn* (a nonstandard setting of No. 56). Data collection was carried out at  $-100^\circ\text{C}$  up to  $2\theta_{\text{max}}$  of  $45^\circ$ . The resolution of the THF molecule was poor, but the  $\text{Ni}_3(\text{dpa})_4\text{Cl}_2$  was refined without difficulty. Details are given in Table 1 and selected interatomic distances in Table 3. Other crystallographic data are given as Supporting Information.

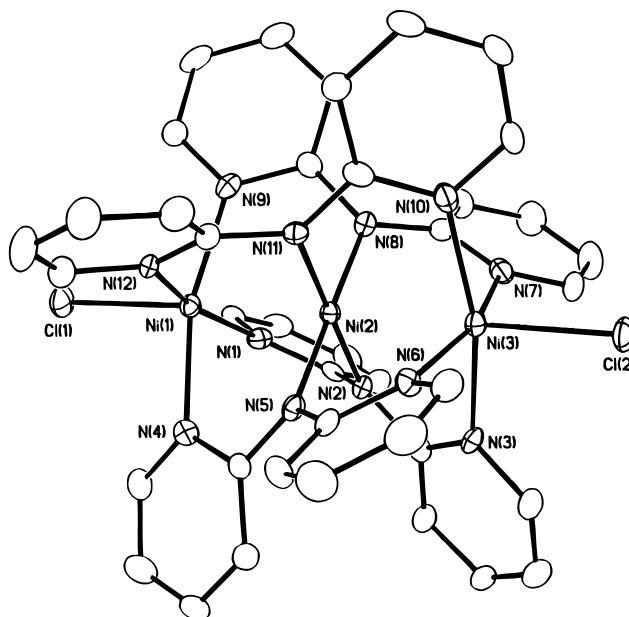
## Results and Discussion

It is pertinent to compare the previously determined structure<sup>2</sup> with those being reported here. For this purpose these will be labeled as follows: **1A** and **1B** denote the two crystallographi-

**Table 4.** Comparison of Metric Parameters Found in  $\text{Ni}_3(\text{dpa})_4\text{Cl}_2$  Compounds

mean values <sup>a</sup>	<b>1A</b>	<b>1B</b>	<b>2</b>	<b>3</b>
Ni···Ni (Å)	2.443[1]	2.431(1)	2.43[8]	2.4172(8)
Ni–Cl (Å)	2.34[5]	2.325(3)	2.34[6]	2.334(2)
Ni–N, central (Å)	1.89[3]	1.88[9]	1.89[3]	1.89[6]
Ni–N, outer (Å)	2.10[3]	2.10[7]	2.09[9]	2.08[8]
overall twist angle (deg)	49.6	53.2	51.0	52.8

<sup>a</sup> Numbers with square brackets are averaged values.

**Figure 1.** Drawing of the molecular structure of  $\text{Ni}_3(\text{dpa})_4\text{Cl}_2$  in  $2 \cdot 2\text{CH}_2\text{Cl}_2$ . Displacement ellipsoids are shown at the 40% level.

cally independent molecules, one on a general position, the other on a 2-fold axis, in the previously reported structure; **2** designates the molecule in  $\text{Ni}_3(\text{dpa})_4\text{Cl}_2 \cdot 2\text{CH}_2\text{Cl}_2$ ; **3** designates the molecule with 2-fold structural symmetry in  $\text{Ni}_3(\text{dpa})_4\text{Cl}_2 \cdot \text{THF}$ . Critical dimensions for each of these four molecules are listed in Table 4, where it is clear that the four are essentially identical. Clearly, whether the molecule is crystallographically required to display 2-fold rotational symmetry or not, it does so. The idealized symmetry in all cases is  $D_4$ .

The Ni–N distances differ considerably for the central and terminal nickel atoms as previously noted.<sup>2</sup> The average values are 1.89 and 2.09 Å, respectively. This is consistent with the view, to be supported (see below) by the interpretation of the magnetic data, that the inner nickel atom is low-spin, while the terminal ones are high-spin. More recently the homologous compound with a chain of five nickel(II) atoms,  $\text{Ni}_5(\text{tpda})_4\text{Cl}_2$ , was reported,<sup>7</sup> and here again the Ni–N distances for the three inner nickel atoms are much shorter (1.904 Å) than those for the two terminal nickel atoms (2.111 Å).

To see if the molecule displays full  $D_4$  symmetry in solution, we examined the  $^1\text{H}$  NMR spectrum. Fortunately, the relative nuclear and electronic relaxation times are such that, despite the paramagnetism (see later) of the molecule, a broadened and strongly shifted, but resolved, spectrum was recorded. This is shown in Figure 2. For a symmetrical molecule the eight pyridyl groups should be equivalent and only four lines should be seen

(4) Pflugrath, J.; Messerschmidt, A. *MADNES*, Munich Area Detector (New EEC) System, Version EEC 11/1/89, with enhancements by Enraf-Nonius Corp., Delft, The Netherlands. A description of MADNES appears in: Messerschmidt, A.; Pflugrath, J. *J. Appl. Crystallogr.* **1987**, *20*, 306.

(5) (a) Kabsch, W. *J. Appl. Cryst.* **1988**, *21*, 67. (b) Kabsch, W. *J. Appl. Cryst.* **1988**, *21*, 916.

(6) *SHELXTL* (version 5.03); Siemens Industrial Automation Inc: Madison WI.

(7) (a) Shieh, S.-J.; Chou, C.-C.; Lee, G.-H.; Wang, C.-C.; Peng, S.-M. *Angew. Chem., Int. Ed. Engl.* **1997**, *36*, 56. (b) Wang, C.-C.; Lo, W.-C.; Chou, C.-C.; Lee, G.-H.; Cheng, J.-M.; Peng, S.-M. *Inorg. Chem.* **1998**, *37*, 4059.

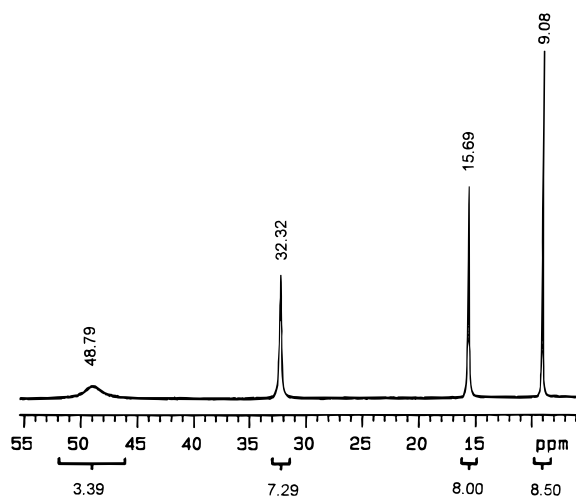


Figure 2. Proton NMR spectrum of  $\text{Ni}_3(\text{dpa})_4\text{Cl}_2$  in  $\text{CD}_2\text{Cl}_2$ .

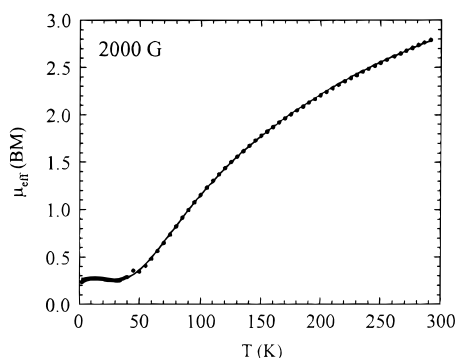


Figure 3. Effective magnetic moments ( $\mu_{\text{eff}}$ , BM) for  $\text{Ni}_3(\text{dpa})_4\text{Cl}_2 \cdot 2\text{CH}_2\text{Cl}_2$  in the temperature range 2–300 K.

with their intensities decreasing with increasing magnitude of the contact shift. This is exactly what is observed.

The third important property of the molecule is its magnetic behavior and what it tells us about the electronic structure of the molecule. It was reported as early as 1968 that the magnetic susceptibility of the compound corresponds to an effective magnetic moment of  $3.7 \mu_B$  at room temperature.<sup>1</sup> It was suggested that this be attributed to a single paramagnetic nickel(II) ion at the center, tetrahedrally coordinated, while the two other nickel(II) ions were assigned square coordination and, hence, make no contribution to the magnetic moment. A later measurement,<sup>2</sup> again only at room temperature, gave a molar magnetic moment of  $3.5 \mu_B$ , which was attributed to two terminal high-spin nickel(II) ions. These authors also reconciled the visible-near-infrared absorption spectrum with the same assignment of spin states.

The results we have obtained do not conflict with the previous interpretation<sup>2</sup> of the room-temperature magnetic susceptibility, but allow more insight, as a result of measuring the temperature dependence. However, there is some significant quantitative disagreement, since we find that the susceptibility at room temperature (300 K) corresponds to a  $\mu_{\text{eff}}$  of only  $2.8 \mu_B$ . Moreover, as shown in Figure 3,  $\mu_{\text{eff}}$  drops steadily to a value of about  $0.3 \mu_B$  at 30–40 K, where it remains down to 2 K. Our interpretation of this is that the two terminal nickel(II) ions, each having  $S = 1$ , are antiferromagnetically coupled ( $-2J = 108 \text{ cm}^{-1}$ ). The fit was performed in the range 10–300 K.<sup>8</sup> The apparent value of  $\mu_{\text{eff}}$  of ca.  $0.3 \mu_B$  between 2 and 30 K is attributable to a paramagnetic impurity.

The final question to be dealt with here concerns the conclusions we can draw (if any) regarding bonding in the  $\text{Ni}_3^{6+}$

chain. Bonding between the metal atoms can arise only from the overlaps of symmetry-matched orbitals. Thus, the three  $d_z^2$  orbitals can combine to form the typical three-center pattern of bonding, nonbonding, and antibonding three-center molecular orbitals, somewhat perturbed by interaction with the  $\sigma$  lone pairs on the axial chlorine orbitals. In a similar way the three  $d_{xz}$ , the three  $d_{yz}$ , and the three  $d_{xy}$  orbitals would all combine into bonding, nonbonding, and antibonding MOs. Overall there would be four bonding, four nonbonding, and four antibonding orbitals. The three  $\text{Ni}^{\text{II}}$  atoms possess a total of  $3 \times 8 = 24$  valence electrons. Thus there are 12 electrons pairs to fill 12 MOs, and there would be no net bonding. However, there would be no unpaired electrons either. This, of course, is consistent with the magnetic susceptibility at 5 K. Thus, we could attribute the increase of magnetic susceptibility as the temperature rises to the population of higher-lying triplet and quintuplet states.

Conversely, we might adopt the suggestion already made, namely, to regard the central nickel atoms as being in a square-planar ligand field that results in a low-spin state, while the two outer five-coordinate nickel ions each in a triplet state are antiferromagnetically coupled. While it is not possible to choose between the two models on the basis of the magnetic data alone, the structure of the molecule lends independent support to the magnetic coupling model. The values of the Ni–N bond distances for the central and terminal nickel atoms fit this model perfectly, whereas it is not clear why the considerable difference between those for the central and the terminal nickel atoms should occur if the covalent but nonbonded model is correct. It must be said that the observations are not necessarily inconsistent with such a model, but we believe that the magnetic coupling model is more likely to be right.

Regardless of which model is correct, it is important that both lead to the same conclusion with regard to the suitability of  $\text{Ni}_n^{2n+}$  chains to be used for “electronic communication” (in whatever experimental way that is to be demonstrated) between the ends of the molecule. Without continuous bonding along the chain, it seems unlikely that this property will be realized and the goal of a “molecular wire” should be sought elsewhere.

**Acknowledgment.** We gratefully acknowledge financial support from the National Science foundation (CHE 96-22589 for K.R.D.). K.R.D. and R.C. also thank The Center For Fundamental Materials at Michigan State University for partial funding of this work and the SQUID magnetometer.

**Supporting Information Available:** X-ray crystallographic files in CIF format for the structure determinations of  $\text{Ni}_3(\text{dpa})_4\text{Cl}_2 \cdot 2\text{CH}_2\text{Cl}_2$  and  $\text{Ni}_3(\text{dpa})_4\text{Cl}_2 \cdot \text{THF}$ . This material is available free of charge via the Internet at <http://pubs.acs.org>.

IC990006T

- (8) The magnetic data were fit by a simple dimer model with the Heisenberg–Dirac–van Vleck Hamiltonian:

$$\chi = \frac{Ng^2\mu_B^2}{3k_B T} \frac{\sum_S S(S+1)(2S+1) \exp(-E(S)/k_B T)}{\sum_S (2S+1) \exp(-E(S)/k_B T)}$$

For two spins,  $S = 1$ , and making allowance for diamagnetism and paramagnetic impurities, this becomes

$$\chi = \frac{2Ng^2\mu_B^2}{k_B T} \frac{e^x + 5e^{3x}}{1 + 3e^x + 5e^{3x}} + \frac{N'\mu_B^2}{k_B T} \chi_{\text{dia}}$$

with  $x = 2J/k_B T$ . This function was fitted with  $R = 0.99997$  using  $2J = -108 \text{ cm}^{-1}$ ,  $g = 2.28$ , and a paramagnetic contribution of about 2.5% of an impurity with  $S = 1/2$ .